JOURNAL OF AGRICULTURAL AND FOOD CHEMISTRY

Article

pubs.acs.org/JAFC

Optimization of Preparation Conditions for Quercetin Nanoemulsions Using Response Surface Methodology

Ayse Karadag,[†,‡] Xiaoqing Yang,[‡] Beraat Ozcelik,[†] and Qingrong Huang*[,‡]

[†]Department of Food Engineering, Faculty of Chemical and Metallurgical Engineering, Istanbul Technical University, 34469 Maslak, Istanbul, Turkey

[‡]Department of Food Science, Rutgers University, 65 Dudley Road, New Brunswick, New Jersey 08901, United States

ABSTRACT: Response surface methodology was used to optimize the conditions for quercetin (QT) nanoemulsion preparations. The parameters to produce stable coarse emulsion formulations, which contain limonene oil, emulsifiers consisting of a Tween 80 and Span 20 mixture (1:1 weight ratio), and a water phase, using high-speed homogenization were identified by using the pseudoternary phase diagram. Subsequently, QT loading was kept constant (0.25%, w/w), and the effects of the oil (10−20%, w/w) and emulsifier (5−15%, w/w) concentrations as well as the homogenization pressure (52−187 MPa) on the particle sizes and emulsion stability were investigated. Experimental data could be adequately fit into a second-order polynomial model with a multiple regression coefficient (R^2) of 0.9171 for the particle size. R^2 values were found to be 0.8545 for the droplet growth ratio during storage and 0.7795 for QT stability. According to the model, major factors affecting particle sizes include the pressure, emulsifier and oil concentrations, and interaction between pressure and oil concentration. The pressure, oil concentration, and interaction terms between the emulsifier and oil concentrations as well as between the pressure and emulsifier concentration had a significant impact on the droplet growth ratio. Regarding the quercetin stability in nanoemulsions, only the oil concentration and interaction term between the oil and emulsifier concentrations had a significant effect. Optimum formulation and conditions for minimum particle size and the highest stability were found at 13% mixed emulsifiers, 17% oil content, and 70 MPa homogenization pressure. This study also suggested that the loading of QT in nanoemulsions could significantly affect the particle sizes and the stability of emulsions depending on the oil:emulsifier ratio in the system.

KEYWORDS: *nanoemulsion, quercetin, response surface model*

INTRODUCTION

Flavonoids are a large group of plant polyphenolic compounds that are commonly distributed in the plant kingdom and largely found in the diet. Among the flavonoids, quercetin (QT, 3,3′,4′,5,7-pentahydroxyflavone) (Figure 1) accounts for the largest percentage of flavonoid intake by diet.[1] Quercetin has exhibited high free radical scavenging activity toward hydroxyl radical, peroxyl, and superoxide anion compared with other flavonoids.[2] Recently, studies reported that quercetin could inhibit proliferation of multiple cancer cell types, including lung cancer cells, colon cancer cells, prostate carcinoma cells, and pancreatic tumor cells. It can promote cancer cell apoptosis at micromolar concentrations.[3] The flavonoid quercetin possesses anti-inflammatory, antiproliferative, and gene expression changing capacities in vitro. Its antioxidative and anti-inflammatory effects have been shown in vivo as well.[4]

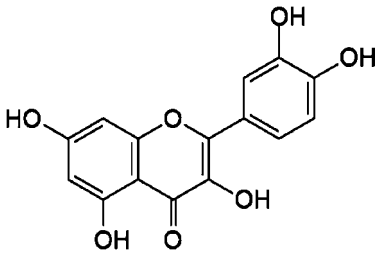

Figure 1. Chemical structure of quercetin.

However, quercetin's low solubility in water (0.17−7.7 μg/mL), artificial gastric juice (5.5 μg/mL), and artificial intestinal juice (28.9 μg/mL) has limited its bioavailability upon oral administration.[5] After quercetin aglycon is received orally, relatively few studies have shown hat it can be detected in plasma and urine.[6] Many approaches have been introduced to enhance the solubility/dispersibility and/or bioavailability of food bioactives through delivery systems such as microemulsions,[5] solid lipid nanoparticles,[3] complexation with cyclodextrin,[7,8] and liposome encapsulation.[9] The combination of lipids and emulsifiers enhances the absorption of quercetin significantly, which is strongly affected by its solubility in the vehicles used for the oral administration.[10] The enhanced bioavailability by the application of microemulsions may be related to the better uptake of nanocarriers through the gastrointestinal tract and the decrease of degradation and/or drug metabolism. Compared with other colloidal vehicles, although microemulsions have numerous advantages, such as thermodynamic stability, simple technology for sample preparation, optical transparency, and low viscosity, microemulsions often require significantly higher contents of oil or surfactant as well as the presence of cosurfactants (short- or medium-chain alcohols), which is generally considered as

Received: September 19, 2012
Revised: January 15, 2013
Accepted: January 18, 2013
Published: January 18, 2013

dx.doi.org/10.1021/jf3040463 | J. Agric. Food Chem. 2013, 61, 2130−2139

undesirable because of potential toxicity issues.[11] For food applications, it is preferred that the delivery vehicles be prepared from food-grade ingredients, which limit the number of surfactants allowed to use. Nonionic surfactants such as sorbitan esters (Tweens or Spans) can be used to deliver food ingredients due to their low toxicity, lack of irritability, and capability to easily form nanoemulsions.[12] Although they have been reported to have minimal toxicity, the biodegradability of many nonionic surfactants raises the concerns of long-term toxicity, especially in chronic use. For this reason, the usage concentration of sorbitan esters in foods must be reduced.[13] In contrast to microemulsions, nanoemulsions can be prepared by reasonable surfactant concentrations (less than 10%) and possess a very small droplet size and high kinetic stability. Therefore, one has to balance the benefits brought by the use of bioactives and potential side effects (e.g., obesity, cardiovascular diseases, etc.) caused by the use of a high amount of lipids and surfactants.[14]

Emulsion-based delivery systems have been used in the food industry to protect active ingredients against harsh conditions, enhance their stability, and mask bad odors and tastes. Nanoemulsions provide high kinetic stability and do not cream (or sediment) because the Brownian motion is larger than the small creaming rate induced by gravity. The internal phases of nanoemulsions supply an excellent reservoir for phytochemicals that need protection and transportation. Their small droplet sizes range from 50 to 200 nm, which is much smaller than the range of 1−100 μm of conventional emulsions, enhancing not only the stability of the emulsions, but also the bioavailability of the encapsulated phytochemicals.[14,15]

Different factors, including process conditions and emulsion composition, influence the physicochemical properties of the nanoemulsions.[16,17] Response surface methodology (RSM) is a collection of mathematical and statistical techniques based on the fit of a polynomial equation to the experimental data, which must describe the behavior of a data set with the objective of making statistical previsions. RSM has a major advantage over the one-factor-at-a-time approach and allows the evaluation of the effect of multiple variables and their interactions on the output variables with a reduced number of experimental trials, development time, and overall cost. It can be well applied when a response or a set of responses of interest are influenced by several variables. The objective is to simultaneously optimize the levels of these variables to attain the best system and optimize the process conditions or product formulation.[16−18] The response surface graphs and contour plots provide a visual aid in examining the effect of variables on each factor and in determining the optimum levels for production of the final product.[19]

The aim of the present study is to prepare quercetin (QT)-loaded nanoemulsions with nonionic food-grade emulsifiers by using high-pressure homogenization and to optimize the pressure and emulsifier and oil concentrations that produce the smallest particle size and greatest stability by using RSM.

MATERIALS AND METHODS

Materials. Quercetin dihydrate (QT) (purity >90%) was obtained from Merck Chemicals. Food-grade limonene oil and medium-chain triacylglycerol (oil, MCT) were kindly provided by the Florida Chemical Co. (Winter Haven, FL) and Stepan Co. (Northfield, IL), respectively. Poly(oxyethylene) (20) sorbitan monooleate (Tween 80, T80), sorbitan monododecanoate (Span 20, S20), ethanol, and sodium azide (NaN_3) were purchased from Sigma-Aldrich Co. (St. Louis, MO). Milli-Q water was used in all experiments.

Solubility of Quercetin. The solubilities of QT in limonene oil, MCT, and oils mixed with emulsifiers (Span 20 and Tween 80) were investigated. An excess amount of QT was added to 3 g of oil, mixed at room temperature and 130 °C for 30 min on a magnetic stirrer, and filtered through a 0.45 μm filter afterward. The filtrate was diluted with ethanol, and UV−vis absorbance at 373 nm was measured with a Cary UV−vis spectrophotometer (Varian Instruments, Walnut Creek, CA) with a 1 cm optical path. The quantity of QT was determined according to the calibration curve of QT (R^2 = 0.997; $y = 0.074x - 0.032$) in ethanol in the concentration range of 2−15 ppm.

Screening of Emulsion Formulations by Construction of a Phase Diagram. Nine different formulations were initially prepared by mixing oil and a surfactant mixture (Tween 80/Span 20, 1:1 weight ratio) with different weight ratios ranging from 1:9 to 9:1 (oil:surfactant). After homogenization by a high-speed homogenizer (Ultra-Turrax T-25 basic, IKA Works Inc., Wilmington, NC) at 24 000 rpm for 5 min, part of the sample was collected in a tube for stability investigation, while the other part was serially diluted in water and treated by high-speed homogenization (HSH). The amount of aqueous phase added was varied to produce a water concentration in the range of 5−90% of the total volume to generate the other points in the phase diagram. All samples were stored at room temperature. After 24 h, the state of the emulsified systems was visually evaluated and classified as physically unstable or stable.[20]

Preparation of Quercetin Nanoemulsions. After determination of the stable emulsion region in the pseudoternary phase diagram, oil-in-water (o/w) nanoemulsions for all experimental conditions (Tables 1 and 2) determined by RSM were prepared as follows: QT was first dissolved in the mixture of limonene oil and Tween 80 at different concentrations, and the solution was mixed with Span 20 and water. The emulsifier used was a 1:1 weight ratio of Tween 80 and Span 20. All formulations contained 0.01 wt % NaN_3 in the final emulsion formulations to inhibit the microbial growth. The premix was homogenized using HSH at 24 000 rpm for 5 min to form a coarse emulsion, followed by high-pressure homogenization (HPH; high-pressure homogenizer, EmulsiFlex-C3, Avestin Inc., Ottawa, Canada) for six cycles at predetermined pressures. The homogenization temperature was set at 25 °C. After homogenization, the emulsions were collected and stored at room temperature; their particle size and stability were analyzed.

Table 1. Uncoded and Coded Independent Variables Used in RSM Design[a]

		coded levels				
independent variable	symbol	$-\alpha$	−1	0	1	$+\alpha$
pressure (MPa)	X_1	52	80	120	160	187
emulsifier concn (%)	X_2	4.95	7	10	13	15.05
oil concn (%)	X_3	9.95	12	15	18	20.05

[a] α = 1.682 for three-factor central composite design. The number of runs is 18 when the center point number is 4.

Particle Size Analysis. The hydrodynamic diameter (z-average) of the emulsion droplets was measured using a photon correlation spectroscopy (PCS)-based BIC 90 plus particle size analyzer equipped with a Brookhaven BI-9000AT digital correlator (Brookhaven Instrument Corp., New York). The samples were diluted approximately 100-fold with Milli-Q water prior to the measurement to prevent multiple scattering and then placed in the cuvette holder, which was kept at a temperature of 25.0 ± 0.1 °C. The light source of the particle size analyzer was a solid-state laser operating at 658 nm with 30 mW power, and the signals were detected by a high-sensitivity avalanche photodiode detector. The normalized field−field autocorrelation function $g(q,t)$ was obtained from the intensity−intensity autocorrelation function, $G(q,t)$, via the Sigert relation.[21,22]

Table 2. Experimental Values of Particle Size and Emulsion Stability of QT Nanoemulsions Obtained from the Central Composite Experimental Design[a]

				decoded values			experimental values		
run no.	coded values			X_1	X_2	X_3	Y_1	Y_2	Y_3
1	−1	−1	−1	80	7	12	155.3	0.960	0.962
2	1	−1	−1	160	7	12	122.2	0.231	0.893
3	−1	1	−1	80	13	12	142.9	0.620	0.883
4	1	1	−1	160	13	12	106.3	0.802	0.744
5	−1	−1	1	80	7	18	123.6	0.915	0.742
6	1	−1	1	160	7	18	109.9	0.387	0.716
7	−1	1	1	80	13	18	117.6	0.341	0.887
8	1	1	1	160	13	18	99.7	0.242	0.834
9	$-\alpha$	0	0	52	10	15	133.5	0.626	0.920
10	$+\alpha$	0	0	187	10	15	116.0	0.060	0.860
11	0	$-\alpha$	0	120	4.95	15	129.6	0.494	0.773
12	0	$+\alpha$	0	120	15.05	15	108.1	0.290	0.976
13	0	0	$-\alpha$	120	10	9.95	159.8	0.636	0.895
14	0	0	$+\alpha$	120	10	20.05	108.7	0.331	0.800
15	0	0	0	120	10	15	111.3	0.388	0.927
16	0	0	0	120	10	15	112.3	0.432	0.842
17	0	0	0	120	10	15	103.1	0.621	0.852
18	0	0	0	120	10	15	110.7	0.511	0.845

[a] X_1 = pressure (MPa), X_2 = emulsifier concentration (%), X_3 = oil concentration (%), Y_1 = particle size (nm) at day 0, Y_2 = droplet growth ratio at day 12, and Y_3 = QT stability ratio at day 14.

Stability of Quercetin Nanoemulsions. An emulsion may become unstable due to a number of processes. In our study, the stability of emulsions was defined in two terms: droplet growth ratio and stability of QT in a nanoemulsion system. Since the QT emulsion in our system tends to aggregate with storage, the droplet size of emulsions at the bottom of the test tubes with time (until day 12) was measured, and the change in size compared to that on the day of preparation was defined as the droplet growth ratio. About 250 μL of emulsion sample was carefully collected using an automatic pipet from the bottom of the test tubes and then diluted 100-fold with Milli-Q water prior to analysis. The stability of QT in the emulsion formulations was determined at days 0, 4, 7, and 14 using a UV−vis spectrophotometer with an absorption wavelength of 373 nm after dilution with ethanol. The change in the UV/vis absorbance of quercetin over time can be used as an indication of QT stability in a nanoemulsion.[21,23]

$$\text{droplet growth ratio} = \frac{\text{particle size at day 12} - \text{particle size at day 0}}{\text{particle size at day 0}} \quad (1)$$

$$\text{QT stability ratio} = \frac{\text{absorbance at day 14}}{\text{absorbance at day 0}} \quad (2)$$

Self-Diffusion Measurements. NMR (nuclear magnetic resonance) measurements were carried out using a Varian VNMRS 400 MHz NMR spectrometer with a 10 A gradient amplifier unit and a 5 mm autoswitchable probe, which was equipped with a z-gradient coil, providing a z-gradient strength of up to 60.78 G/cm. Diffusion measurements were carried out using the bipolar pulse gradient stimulated echo technique. The experiments were performed by varying the gradient strength along the z-axis (G_z) while keeping the gradient pulse duration (δ) and the diffusion delays (Δ) constant. The echo intensity decay as the value of G_z increases is given by

$$I(G_z) = I(0)\exp[-D\gamma^2\delta^2 G_z{}^2(\Delta - \delta/3)] \quad (3)$$

where D is the self-diffusion coefficient of the species responsible for the spin−echo decay, $I(0)$ is the echo intensity in the absence of any pulse gradient, and γ is the gyromagnetic constant of the observed nucleus, which is 26 752 for H. The applied field gradient strength (G) was calibrated before each experiment. The temperature of the sample was maintained at 25 °C by a built-in variable-temperature control unit managed by the spectrometer software. Spectra for 15 different values of G, which were from 0.74 to 40.81 G/m in 15 steps, were recorded for each sample, and the duration of the gradient (δ) was kept at 2 ms in all the diffusion experiments.

Experimental Design. After the stable emulsion region in the pseudoternary phase diagram was determined, RSM was used to study the effect of the independent variables, such as pressure (X_1), concentration of the emulsifier (X_2), and concentration of the oil (X_3), on the dependent variables, which include the particle size (Y_1), droplet growth ratio (Y_2), and stability of QT (Y_3) in nanoemulsions. The QT loading was set at 0.25% (w/w) for all formulations. The coded and uncoded independent variables used in the RSM design are listed in Table 1. A five-level central composite rotatable design was used for the RSM studies, and 18 experimental settings were generated with 3 factors as shown in Table 2. Individual experiments were carried out in randomized order. Optimization of the emulsion formulations in terms of pressure and oil and emulsifier concentrations was achieved by an evaluation of the contour plots. A second-order polynomial equation was used to express predicted responses (particle size, Y_1; droplet growth ratio, Y_2; stability of QT in an emulsion, Y_3) as a function of the independent variables as follows:

$$Y_i = a_0 + a_1X_1 + a_2X_2 + a_3X_3 + a_{12}X_1X_2 + a_{13}X_1X_3 + a_{23}X_2X_3 + a_{11}X_1{}^2 + a_{22}X_2{}^2 + a_{33}X_3{}^2 \quad (4)$$

where X_i represent the independent variables, a_0 is a constant, a_i, a_{ii}, and a_{ij} are the linear, quadratic, and interactive coefficients, respectively. The significance of the estimated regression coefficient for each response variable was assessed at a probability (p) of 0.05. The experimental design matrix data analysis was performed using Statistica 8 (StatSoft, Inc., 2007).

Statistical Analysis. The experimental data were analyzed by multiple regressions to fit the second-order polynomial equation to all independent variables. The goodness of fit of the model was evaluated by the coefficient determination (R^2) and the analysis of variance (ANOVA). To visualize the relationships between the responses and the independent variables, the surface response and contour plots of the fitted polynomial regression equations were generated using Statistica 8 software. The optimal conditions for the targeted responses

Table 3. Solubility of Quercetin (mg/g) in Limonene Oil and MCT and Their Combination with Emulsifiers Tween 80 (T80) and Span 20 (S20)[a]

			mixed with an emulsifier				
			T80:oil, w/w				S20:oil, w/w
oil type	at room temperature	at 130 °C	1:1	1:2	1:4	1:6	1:2
limonene oil	0.617 ± 0.098	2.29 ± 0.47	39.47 ± 6.41	27.24 ± 3.65	19.82 ± 1.43	13.16 ± 2.27	1.23 ± 0.02
MCT	0.279 ± 0.057	2.09 ± 0.54	*b*	*b*	*b*	*b*	1.972 ± 0.39

[a]The data represent the average of three measurements carried out in duplicate samples. [b]MCT and T80 do not mix.

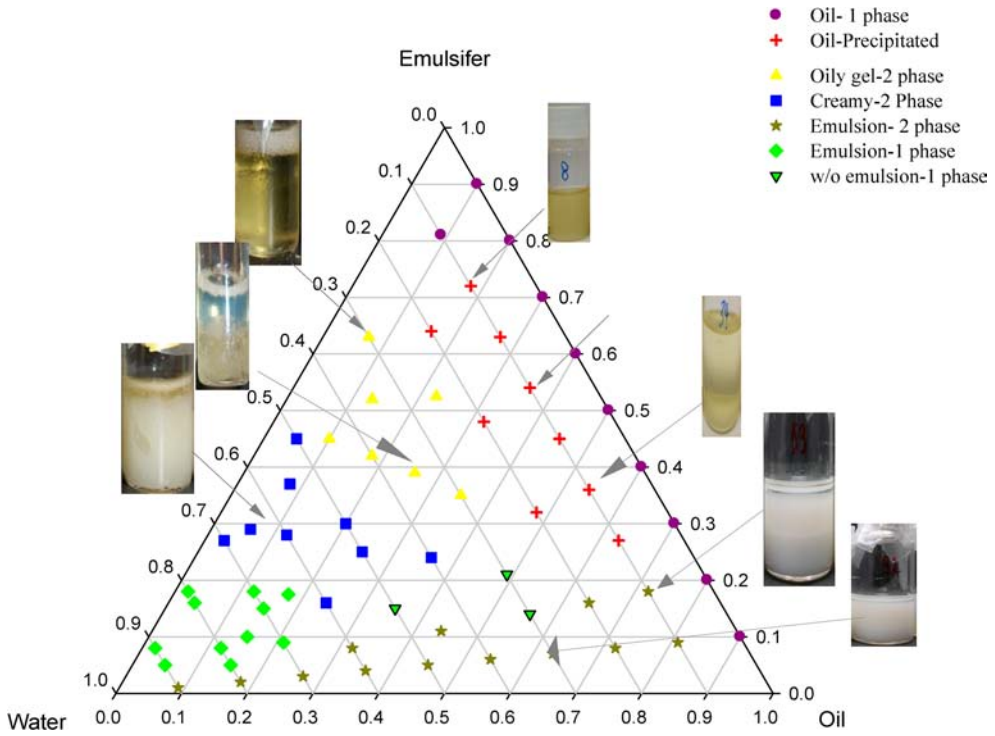

Figure 2. Pseudoternary phase diagram and stability of the limonene oil/emulsifier (S20/T80,1:1, w/w)/water system homogenized by HSH.

were generated by the Modde 8.0 (Umetrics) software to validate the model.

RESULTS AND DISCUSSION

Solubility of Quercetin. The solubility of QT was determined using two kinds of oil, namely, limonene oil and MCT, and their combinations with emulsifiers Tween 80 and Span 20 at room temperature and at 130 °C. At room temperature, the solubility of QT in limonene oil was around 2 times higher than that of QT in MCT. When the oil was heated to 130 °C for 30 min, the solubility of QT in both oils increased to the same levels. The solubility was drastically increased when limonene oil was mixed with Tween 80 at room temperature depending on the emulsifier concentration. QT solubility increases when Tween 80 is mixed with limonene oil in different concentrations. Limonene oil and MCT were also mixed with Span 20 in a ratio of 1:2 (S20:oil, w/w), and the solubility values were considerably lower than that of limonene oil mixed with T80 (Table 3). Since the solubility of QT is the highest in limonene oil compared with other common food-grade oils such as MCT, sunflower oil, vegetable oil, etc., limonene oil was chosen as the oil phase in the following formulations. A number of studies have shown that the solubility of highly hydrophobic compounds in oil phases can be increased by using mixtures of hydrophilic and lipophilic surfactants.[24,25] The ratio of hydrophilic (Tween 80 with a hydrophilic−lipophilic balance (HLB) value of ∼18) to lipophilic (Span 20 with an HLB value of ∼6) surfactant was chosen as 1:1 (w/w). Because it was found that when limonene oil was used as the oil phase, the emulsion formulations prepared with the mixture of Tween 80 and Span 20 having an HLB value of 12 produced the smallest droplet sizes.[26,27] In another study the stability and formation (with a high-pressure homogenizer) of orange oil/water nanoemulsions in the presence of mixtures of nonionic surfactants, having different HLB values, varying their type and concentration, were evaluated. The results also showed that the optimal HLB range of the surfactant mixtures to obtain stable o/w nanoemulsions was around 12.[27]

Screening of Emulsion Formulations by Constructing a Phase Diagram. Nanoemulsions were prepared by application of HSH to produce a coarse emulsions, which were then subjected to HPH to produce the secondary nanoscale emulsions. The stability of the coarse emulsions was evaluated for different formulations in terms of emulsifier and oil contents and reported in the pseudoternary phase diagram, shown in Figure 2. Pseudoternary phase diagrams are frequently used, especially in the formulation of self-emulsifying drug delivery systems, which are thermodynamically stable emulsions.[20] In the triangular phase diagram of Figure 2, the

dx.doi.org/10.1021/jf3040463 | J. Agric. Food Chem. 2013, 61, 2130−2139

Table 4. Analysis of Variance of the Regression Coefficients of the Fitted Quadratic Equations for the Particle Size and Stability (Droplet Growth Ratio and Quercetin Stability) of Nanoemulsions

dependent variable	independent variable	coefficient	p value	model fit
particle size	pressure	−1.4006	0.0036[a]	R^2 = 0.9171
	pressure^2	2.71×10^{-3}	0.0357[b]	
	emulsifier concn	−8.7067	0.0141[b]	
	(emulsifier concn)^2	2.59×10^{-1}	NS[c]	
	oil concn	−36.324	0.0019[a]	
	(oil concn)^2	8.64×10^{-1}	0.0073[a]	
	pressure × emulsifier concn	8.17×10^{-3}	NS	
	pressure × oil concn	-3.98×10^{-2}	0.0498[b]	
	emulsifier concn × oil concn	1.68×10^{-1}	NS	
	constant	563.3528	0.0000[a]	
lack of fit			0.1355	
droplet growth ratio	pressure	-1.41×10^{-2}	0.0110[b]	R^2 = 0.8545
	pressure^2	-1.07×10^{-5}	NS	
	emulsifier concn	8.17×10^{-3}	NS	
	(emulsifier concn)^2	1.04×10^{-4}	NS	
	oil concn	1.19×10^{-3}	0.0460[b]	
	(oil concn)^2	3.68×10^{-3}	NS	
	pressure × emulsifier concn	1.39×10^{-3}	0.0188[b]	
	pressure × oil concn	-8.30×10^{-5}	NS	
	emulsifier concn × oil concn	-1.32×10^{-2}	0.0460[b]	
	constant	1.8343	0.0025[a]	
lack of fit			0.2760	
QT stability ratio	pressure	-1.62×10^{-3}	NS	R^2 = 0.7795
	pressure^2	-2.51×10^{-7}	NS	
	emulsifier concn	-7.01×10^{-2}	NS	
	(emulsifier concn)^2	-5.43×10^{-4}	NS	
	oil concn	-4.71×10^{-2}	0.0471[b]	
	(oil concn)^2	-1.61×10^{-3}	NS	
	pressure × emulsifier concn	-1.01×10^{-4}	NS	
	pressure × oil concn	1.32×10^{-4}	NS	
	emulsifier concn × oil concn	6.82×10^{-3}	0.0201[b]	
	constant	1.7503	0.0000[a]	
lack of fit			0.2714	

[a]Statistically significant at $p < 0.01$. [b]Statistically significant at $p < 0.05$. [c]Not significant ($p > 0.05$).

first axis represents water, the second limonene oil, and the third the emulsifier mixture of Span 20 and Tween 80 at a fixed ratio (1:1, w/w). In the present study, the pseudoternary phase diagram was used as a compositional map for the identification of the optimal conditions to obtain kinetically stable emulsions in terms of minimization of the amount of emulsifiers to be employed. Nine different samples were initially prepared by mixing only the emulsifier and oil at different ratios (from 1:9 to 9:1), which on the diagram are located on the right side of the triangle, and homogenized by HSH. The other points reported in the diagram are generated by the serial water dilutions of the original nine mixtures. Twenty-four hours after preparation, the state of the emulsified system was visually evaluated and classified. By the addition of water into the oil and emulsifier mixtures, precipitation at the bottom of the tube was observed when the water content was 10−20% and the oil content was 15−65%. The addition of more water until it hit 50% and when the oil content was lower than 50% generated an oily gel phase which had separated 24 h after preparation.While the water content increased to 70% in the presence of an emulsifier content greater than 25% and up to 30% oil content, an unstable creamy phase was observed which showed two layers. When the oil content was between 35% and 55% and the emulsifier content was 15−20%, a stable water-in-oil (w/o) emulsion region was observed as well. A stable o/w emulsion phase occurred when the oil content was lower than ≤30% and the emulsifier content was lower than <20% (Figure 2). The stable emulsion region found in the pseudoternary phase diagram was further processed by HPH, and the effect of independent variables (pressure, emulsifier and oil concentrations) on the particle size, droplet growth ratio, and QT stability in nanoemulsion formulations was studied by using response surface methodology.

Analysis of the Response Surface Model. *Fitting the Models.* The particle size and stability values of the QT nanoemulsions obtained from all the experiments are shown in Table 2. The experimental data were used to calculate the coefficients of the quadratic polynomial equations, which were used to predict the values of particle size and stability of the emulsions. Since the maximum droplet size changes for QT nanoemulsions occurred on the 12th day, the droplet size change of the 12th day was used in the response surface model. Changes in the QT stability of emulsions on the 14th day were used in the experimental model.

ANOVA in Table 4 indicated that quadratic polynomial models were adequate for the prediction. The models showed no lack of fit because p values for the particle size, emulsion droplet growth, and QT stability (0.1355, 0.2760, and 0.2714)

dx.doi.org/10.1021/jf3040463 | J. Agric. Food Chem. 2013, 61, 2130−2139

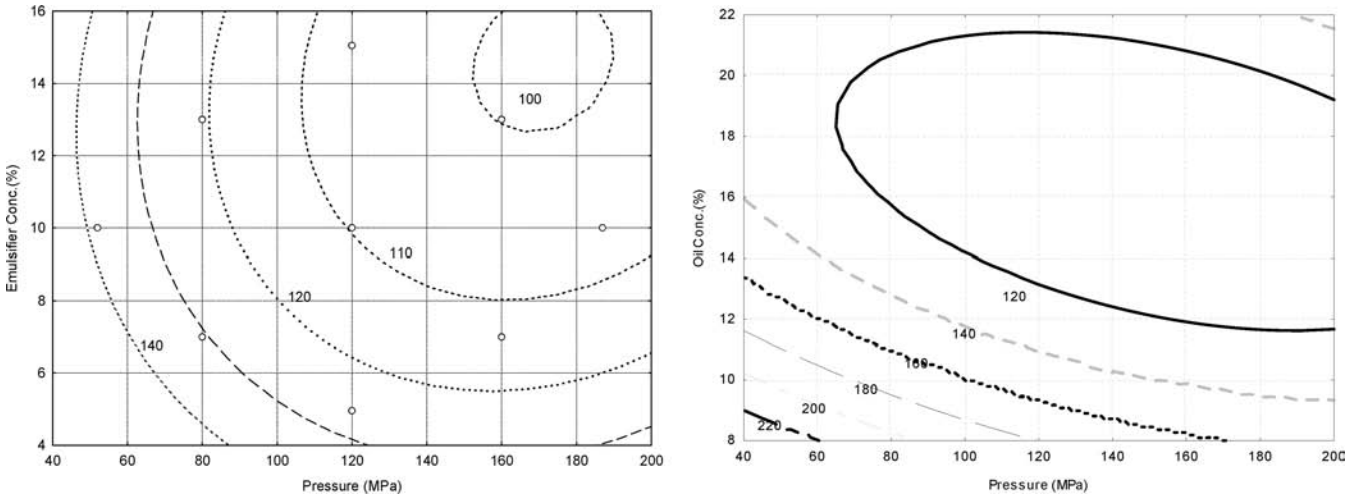

Figure 3. Contour plots of the particle sizes (nm) of the nanoemulsions as a function of pressure and emulsifier concentration (%) (a) at an oil concentration of 15% and (b) at an emulsifier concentration of 10%.

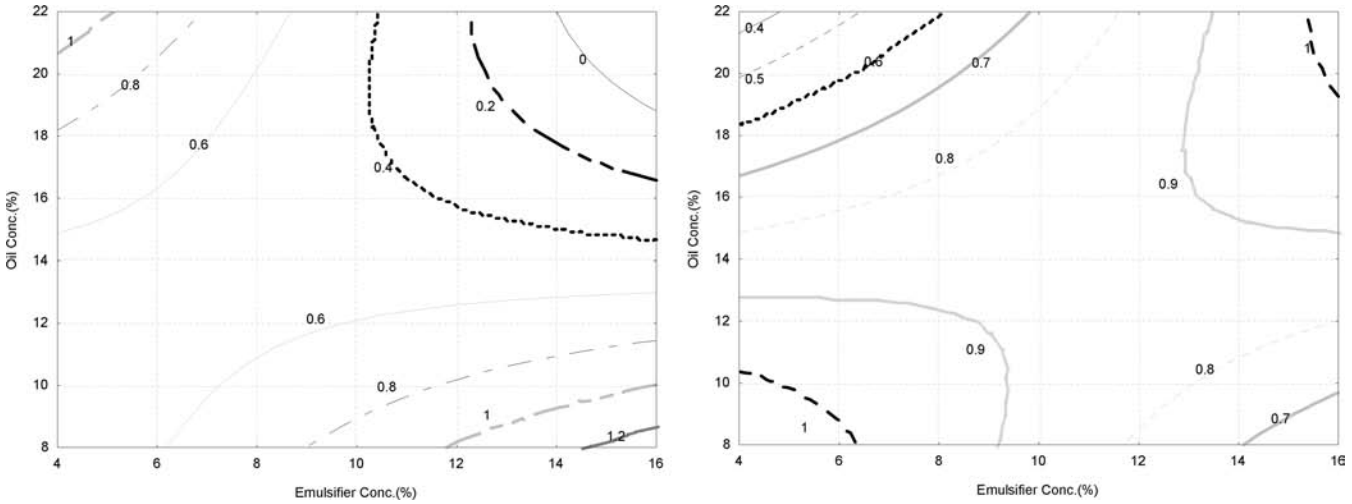

Figure 4. Contour plots of droplet growth (a) and quercetin stability (b) of the nanoemulsions as a function of emulsifier and oil concentrations (%) at a pressure of 120 MPa.

were higher than $p > 0.05$ and the coefficients of multiple determinations, R^2, of 0.9171, 0.8545, and 0.7794 all indicate that the models fit the experimental data points. For any of the terms in the models, a small p value would indicate a more significant effect on the respective response variables. The linear terms of oil concentration and homogenization pressure ($p < 0.01$) and emulsifier concentration ($p < 0.05$), quadratic terms of oil concentration ($p < 0.01$) and homogenization pressure ($p < 0.05$), and interactive terms of pressure and oil concentration ($p < 0.05$) had a significant effect on the particle size of the nanoemulsions. The shear forces and turbulence, which are produced during homogenization and are pressure dependent, would affect the particle sizes and size distributions. Our results agreed with other studies showing that the increased emulsifier concentration and pressure resulted in a decrease of the particle sizes.[16,17,28,29]

At constant oil content, increasing either the emulsifier content or pressure had a tendency to produce smaller droplets. Up to a certain level of oil content, the particle size became smaller at increased pressures; beyond that level of oil concentration, the particle size was not affected by a pressure change. This trend might be expected because the increased pressure would cause larger oil droplets to rupture into smaller droplets, and there should be a larger amount of emulsifier present to cover freshly formed droplet surfaces during homogenization[30] (Figure 3).

The linear terms of oil concentration and homogenization pressure had a significant effect ($p < 0.05$) on the particle size stability of the nanoemulsions. Figure 4 shows the effect of the oil and emulsifier concentrations on the droplet growth ratio and quercetin stability in nanoemulsions. Interaction between these two componenets appeared as saddle surfaces, where particle size stability increased (smaller droplet growth ratio values) when the emulsifier and oil contents were above ~10% and 15%, respectively, and decreased (larger droplet growth ratio values) when either the emulsifier or oil content was lower. The relation between particle size stability and emulsifier content can be explained by the need for an interfacial emulsifier layer aound the droplets to prevent their flocculation or coalescence during storage. The interactions between emulsifier concentration and pressure and oil concentration had a significant effect on droplet growth ($p < 0.05$). The droplet growth ratio at the bottom of the sample bottles was decreased by increased pressure, meaning initially smaller

dx.doi.org/10.1021/jf3040463 | J. Agric. Food Chem. 2013, 61, 2130−2139

Table 5. Particle Sizes of Nanoemulsions Loaded with Different Amounts of QT[a]

		particle size (nm)				
			QT-loaded samples			
emulsifier concn (%)	oil concn (%)	blank samples	0.1% (w/w)	0.25% (w/w)	0.4% (w/w)	0.8% (w/w)
10	5	69.3 ± 2.1	*b*	220.7 ± 11.3	*b*	*c*
10	10	89.0 ± 3.2	93.2 ± 0.4	168.9 ± 12.6	196.5 ± 4.5	*c*
10	20	99.3 ± 8.9	103.9 ± 2.0	101.7 ± 4.7	103.9 ± 2.0	*c*
10	30	116.9 ± 3.1	*b*	124.1 ± 0.9	*b*	*c*
20	10	69.3 ± 0.7	86..9 ± 0.2	175.5 ± 1.3	178.3 ± 23.7	251.7 ± 15.1

[a]The process condition applied for HSH was 3 min at 24 000 rpm, and those for HPH were 120 MPa and six cycles at 25 °C. The data represent the avarage of three measurements carried out in duplicate samples. [b]The experiment was not carried out. [c]The formulation was not prepared because the amount of QT cannot be loaded.

particles were grown more slowly, and this result was in agreement with the fndings of others[31] (Table 4).

To test the stability of quercetin in nanoemulsions, the samples were taken only from the upper level of the sample bottles for UV/vis measurement. The linear term of oil concentration and the interaction of emulsifier and oil concentrations had a significant effect on QT stability ($p < 0.05$) (Table 4). The model equations for the responses only with significant factors (independent variables) can be written as follows:

$$Y_1 = 563.35 - 1.40X_1 - 8.70X_2 - 36.32X_3 - (3.98 \times 10^{-2})X_1X_3 + (2.71 \times 10^{-3})X_1^2 + 0.86X_3^2 + 0.17X_2X_3 \quad (5)$$

$$Y_2 = 1.83 - 0.14X_1 + (1.19 \times 10^{-3})X_3 + (1.39 \times 10^{-3})X_1X_2 - (1.32 \times 10^{-2})X_2X_3 \quad (6)$$

$$Y_3 = 1.75 - (4.71 \times 10^{-2})X_3 + (6.82 \times 10^{-3})X_2X_3 \quad (7)$$

Verification of the Model. The optimal conditions for the targeted responses were generated by the Modde 8.0 (Umetrics) software. After that, at the optimal conditions (pressure 70 MPa, 13% emulsifier content, and 17% oil content), nanoemulsions were prepared. The predicted values for the responses are as follows: 116.4 nm for particle size, 0.2966 for droplet growth ratio, and 0.9075 for QT stability. At these conditions, the experiments were carried out and the particle size was measured to be 119.7 nm, 0.3074 for droplet growth ratio, and 0.8764 for QT stability, which were satisfactorily close to the values predicted by the model.

Quercetin Loading. Some emulsion formulations in the stable region of the pseudoternary phase diagram were loaded with different amounts of QT, and their particle sizes were compared to those of the blank samples (Table 5). First, QT was dissolved in limonene oil and T80 and mixed for 24 h on a magnetic stirrer for complete solubilization; after that the oil phase was mixed with S20 and water and homogenized by HSH and HPH, respectively. The process condition applied for HSH was 3 min at 24 000 rpm, and those for HPH were 120 MPa and six cycles at 25 °C.

For blank samples, when the emulsifier content was kept constant, the samples with higher oil content had a larger particle size (Table 5). More oil content indicates more oil/water interface to cover, and the emulsifier content in the system could not be enough to cover the newly formed droplets, which may cause an increase in the droplet size. This result was in agreement with previous studies.[28,32] However, the samples loaded with QT did not follow the same trend. The particle size mostly depended on the oil concentration and amount of QT dissolved in the system. For the formulations including the same amount of emulsifiers and loaded with the same amount of QT, the particle size became smaller with increasing oil content. When the oil:emulsifier ratio was low, the higher amount of QT in the formulation resulted in larger particle sizes. Although when the oil:emulsifier ratio is high, the change in the particle size may not depend on the amount of QT (Table 2). Increased concentration of the dispersed phase would result in more oil droplets for QT crystals to be accumulated in without affecting the droplet size.

It has been shown that hydrophobic antioxidants in oil-in-water emulsions have a tendency to concentrate at the interfacial membrane where the oxidation is supposed to occur, which increases their effectiveness against oxidation.[33] Quercetin, as a hydrophobic antioxidant, may accumulate both in the oil phase and at the oil/water droplet interface. However, when the dispersed phase concentration is lower and there is less oil/water interface to be occupied by QT, QT accumulates on the available area and might make the oil droplets larger. The enhancement of quercetin absorption by solid nanoparticles was previously studied, and it was also proposed that since quercetin is mostly dissolved in the surfactants in their system, large amounts of surfactants arranged along the interface between water and lipid, the drug incorporation model should fit the core−shell model with a drug-enriched shell.[3] In another study, QT was proven to interact with the micelles by means of hydrophobic interactions.[34] Above a critical concentration, addition of QT into an oil-in-water emulsion caused a significant decrease in the interfacial area of the droplets.[35] It was proposed that, once all the micelles in the aqueous phase are saturated, QT might interact with emulsifier molecules bound to the oil droplet interface, thus favoring the partial coalescence of the newly formed oil droplets and leading to a subsequent decrease of the dispersion state (lower values of interfacial area and larger droplet size).

Another interesting result was that when a formulation was loaded with a smaller amount of QT, it was less stable than one loaded with a greater amount of QT without a dependence on its initial particle size. When the same formulation (oil/emulsifier/water, 10:10:80) was loaded with 0.1% and 0.4% QT, the emulsions loaded with less QT which had a particle size almost equal to that of the blank samples on the day of preparation showed clear phase separation on day 2, whereas the emulsion loaded with 0.4% QT stayed stable with no change in the particle size (Figure 5).

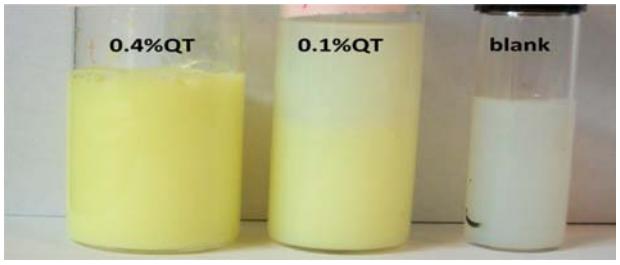

Figure 5. Stability of the emulsions with different quercetin contents on day 2. The composition of the emulsions is 10:10:80 for oil/emulsifier/water.

The stability of the blank emulsion and the systems loaded with hydrophobic compounds will be different. It has been found that hydrophobic bioactive components may form crystals in emulsion-based delivery systems during storage which sediment to the bottom.[25,36] In practice, due to supersaturation, it is often possible to dissolve a greater amount of a crystalline material in a solvent than CS* (the equilibrium solubility) so that the material is fully dissolved below this level, but forms crystals above it.[36] Nevertheless, the system could persist in this metastable supersatutared state for some time before any crystallization is observed due to the presence of activation energies associated with nucleus formation that must be overcome. The height of the activation energy depends on the ability of crystal nuclei to be formed that are stable enough to grow into crystals. At present, little is understood about the origin of nucleation in oil-in-water emulsions and about the consequences for the stability and functional performance of emulsion-based delivery systems. Once nuclei have been formed in a particular location within an emulsion, they may grow into crystals. The size, shape, and location of crystals in an emulsion will affect its physical stability and functional performance.[25,36]

In our system, similar to the study of Li and others,[25] we also observed the presence of a thin yellow layer at the bottom of the nanoemulsion with storage, which might suggest that (i) nucleation and crystal growth occurred directly in the aqueous phase or (ii) nucleation and crystal growth occurred in the oil phase or at the oil−water interface and then the crystals moved into the aqueous phase. In our study, the systems loaded with a higher amount of QT showed increased stability, which might be explained by the mechanism that crystals are unable to move to the droplet surface from the interior of the lipid droplet, because the crystal network formed in the droplet prevents their movement. An estimate of whether the crystals can reach the interface can be given by the ratio t_I/t_N:

$$\frac{t_I}{t_N} = 6\Phi\frac{r_c^2}{r_d^2} \quad (8)$$

Here, t_I is the time required for the crystals to reach the interface, t_N is the time required for network formation, r_c is the radius of the crystal, and r_d is the radius of the lipid droplet. This equation highlights that the lower the crystal concentration within the oil phase the more chance the crystals have to reach the droplet surface. In practice, there will be a minimum crystal concentration required for network formation. If the crystal concentration is below this value, the crystals may aggregate but they may still be able to move to the droplet surface. This critical concentration will depend on the shape of the crystals and the strength of the attractive forces between them.[36]

In our system, the particle size of oil droplets loaded with more QT was larger, and the droplets were more stable to sedimentation compared to the system with smaller droplets loaded with less QT. According to eq 8, the formation of a crystal network that prevents crystals from moving to the interface and eventually to the aqueous phase where they form larger crytal clusters requires a critical crystal concentration, and crystals in the larger sized droplets more likely form the network than the smaller sized droplets. Further work is clearly needed to better understand the influence of quercetin loading, particle size, and the constituents of emulsion (e.g., oil type and concentration and surfactant type and concentration) on the crystal formation and stability of nanoemulsions.

QT loading in this study could be as high as 0.8% for the formulation of 10:20:70 (oil:emulsifier:water). The QT loading in the emulsion system in the literature was found to be 0.043%[11] and 0.065%[37] and that in the liposome system to be 0.5%,[9] where solvent mixtures were used to dissolve QT. A 0.4% QT loading was achieved in a microemulsion system where the initial concentration ratio of oil (ethyl oleate) to surfactant (Tween 80) to cosurfactant (dehydrated ethanol) was 7:48:45.[5]

Self-Diffusion Measurements. The diffusion coefficient of pure limonene (D^O_0) was determined to be 16.1×10^{-10} m^2/s, while the diffusion coefficient of pure water (D^W_0) was 22.0×10^{-10} m^2/s. Relative diffusion coefficients were obtained by dividing D_W and D_O in the nanoemulsions by D^W_0 and D^O_0. In this study, nanoparticles were produced by the combination of high-speed and high-pressure homogenization. Therefore, both lipid diffusion and Brownian motion (random particle movements) for all the oil droplets (nanoparticles) were present in all the samples. Consequently, fluctuations for the diffusion coefficient measurements of the lipid particles were observed in all the NMR experiments, so only the D values for the aqueous phase are reported in this paper. The relative D values for water are shown in Table 6. The initial objective of our NMR studies was to determine the location of encapsulated quercetin. Our results fail to achieve this goal at this point, but it is proven that the discrete particle structures occurred in these formaulations because the relative D value of water was significantly larger than that of the oil. It has been proven that if the relative diffusion coefficient of water is more than 10 times larger than that of the oil (limonene), discrete particles are expected rather than other structures such as a bicontinuous structure.[38]

Table 6. Relative Diffusion Coefficient Values of Water in a Nanoemulsion Loaded with Quercetin at 10% Emulsifier Content and Calculated from NMR Results at 25 °C

oil concn (%)	D_W/D^W_0	oil concn (%)	D_W/D^W_0
5	0.752	30	0.569
10	0.657	40	0.558
20	0.512		

In summary, stable QT limonene oil-in-water nanoemulsions were prepared by using a nonionic emuslifier mixture and applying high-pressure homogenization. The kinetically stable emulsion range was first identified by using the pseudoternary phase diagram to minimize the amount of emulsifier. After that, in the range where a stable coarse emulsion occurred, RSM was applied to predict the effects of the changes in emulsifying

conditions (pressure and oil and emulsifier concentrations) within the experimental ranges on the particle size and stability of QT emulsions. The independent factors of homogenization pressure and oil and emulsifier concentrations and the quadratics of pressure and oil concentration had a significant effect on the particle size of the nanoemulsions. Concurrently, the independent variable of oil concentration and the interaction between oil and emulsifier concentrations had a significant effect on the stability of QT in nanoemulsions. This study also showed that the particle size of the droplets changes with the QT loading and the oil to emulsifier ratio in the formulation. When the amount of oil in the system was low, increasing the QT loading resulted in an increase of the particle size. However, when there was a high amount of oil in the system, the QT loading did not affect the particle size. When the emulsion formulation was loaded with less QT, it was less stable than the same emulsion formulation loaded with a high amount of QT, regardless of the initial particle size. We suggest that there should be a minimum QT concentration in the oil droplets to form a network that prevents the movement of quercetin. Further work is clearly needed to better understand the influence of the quercetin loading, particle size, and constituents of the emulsion (e.g., oil type and concentration and surfactant type and concentration) on the crystal formation and stability of nanoemulsions.

AUTHOR INFORMATION

Corresponding Author

*Phone: (848) 932-5514. Fax: (732) 932-6776. E-mail: qhuang@aesop.rutgers.edu.

Funding

This work was supported by the U.S. Department of Agriculture and Food Research Initiative (USDA-AFRI; Grant 2009-65503-05793).

Notes

The authors declare no competing financial interest.

REFERENCES

(1) Wach, A.; Pyrzynska, K.; Biesaga, M. Quercetin content in some food and herbal samples. *Food Chem.* **2007**, *100*, 699−704.

(2) Casagrande, R.; Georgetti, S.; Verri, W.; Jabor, J.; Santos, A.; Fonseca, M. Evaluation of functional stability of quercetin as a raw material and in different topical formulations by its antilipoperoxidative activity. *AAPS PharmSciTech* **2006**, *7*, E64−E71.

(3) Li, H.; Zhao, X.; Ma, Y.; Zhai, G.; Li, L.; Lou, H. Enhancement of gastrointestinal absorption of quercetin by solid lipid nanoparticles. *J. Controlled Release* **2009**, *133*, 238−244.

(4) Boots, A. W.; Haenen, G. R. M. M.; Bast, A. Health effects of quercetin: From antioxidant to nutraceutical. *Eur. J. Pharmacol.* **2008**, *585*, 325−337.

(5) Gao, Y.; Wang, Y.; Ma, Y.; Yu, A.; Cai, F.; Shao, W.; G., Z. Formulation optimization and in situ absorption in rat intestinal tract of quercetin-loaded microemulsion. *Colloids Surf, B* **2009**, *71*, 306−314.

(6) Erlund, I. Review of the flavonoids quercetin, hesperetin, and naringenin. Dietary sources, bioactivities, bioavailability, and epidemiology. *Nutr. Res. (N. Y., NY, U. S.)* **2004**, *24*, 851−874.

(7) Zheng, Y.; Chow, A. H. L. Production and characterization of a spray-dried hydroxypropyl-β-cyclodextrin/quercetin complex. *Drug Dev. Ind. Pharm.* **2009**, *35*, 727−734.

(8) Lucas-Abellán, C.; Fortea, I.; Gabaldón, J. A.; Núñez-Delicado, E. Encapsulation of quercetin and myricetin in cyclodextrins at acidic pH. *J. Agric. Food Chem.* **2007**, *56*, 255−259.

(9) Zhang, Y.; Zhang, Y.; Pan, Y.; Wang, J.; Zhang, L.; Long, B.; Liu, X. Study on distribution of liposome nanoparticles loaded quercetin in mice. *Nanoscience* **2006**, *11*, 89−94.

(10) Azuma, K.; Ippoushi, K.; Ito, H.; Higashio, H.; J., T. Combination of lipids and emulsifiers enhances the absorption of orally administered quercetin in rats. *J. Agric. Food Chem.* **2002**, *50*, 1706−12.

(11) Rogerio, A. P.; Dora, C. L.; Andrade, E. L.; Chaves, J. S.; Silva, L. F. C.; Lemos-Senna, E.; Calixto, J. B. Anti-inflammatory effect of quercetin-loaded microemulsion in the airways allergic inflammatory model in mice. *Pharm. Res.* **2010**, *61*, 288−297.

(12) McClements, D. J.; Rao, J. Food-grade nanoemulsions: Formulation, fabrication, properties, performance, biological fate, and potential toxicity. *Crit. Rev. Food Sci. Nutr.* **2011**, *51*, 285−330.

(13) Lawrence, M. J.; Rees, G. D. Microemulsion-based media as novel drug delivery systems. *Adv. Drug Delivery Rev.* **2000**, *45*, 89−121.

(14) Qingrong, H.; Hailong, Y.; Qiaomei, R. Bioavailability and delivery of nutraceuticals using nanotechnology. *J. Food Sci.* **2010**, *75*, R50−57.

(15) Gutiérrez, J. M.; González, C.; Maestro, A.; Solè, I.; Pey, C. M.; Nolla, J. Nano-emulsions: New applications and optimization of their preparation. *Curr. Opin. Colloid Interface Sci.* **2008**, *13*, 245−251.

(16) Yuan, Y.; Gao, Y.; Mao, L.; Zhao, J. Optimisation of conditions for the preparation of β-carotene nanoemulsions using response surface methodology. *Food Chem.* **2008**, *107*, 1300−1306.

(17) Anarjan, N.; Mirhosseini, H.; Baharin, B. S.; Tan, C. P. Effect of processing conditions on physicochemical properties of astaxanthin nanodispersions. *Food Chem.* **2010**, *123*, 477−483.

(18) Bezerra, M. A.; Santelli, R. E.; Oliveira, E. P.; Villar, L. S.; Escaleira, L. A. Response surface methodology (RSM) as a tool for optimization in analytical chemistry. *Talanta* **2008**, *76*, 965−977.

(19) Ozcelik, B.; Karadag, A.; Cinbas, T.; Yolci, P. Influence of extraction time and different sage varieties on sensory characteristics of a novel functional beverage by RSM. *Food Sci. Technol. Int.* **2009**, *15*, 111−118.

(20) Donsì, F.; Senatore, B.; Huang, Q.; Ferrari, G. Development of novel pea protein-based nanoemulsions for delivery of nutraceuticals. *J. Agric. Food Chem.* **2010**, *58*, 10653−10660.

(21) Wang, X.; Jiang, Y.; Wang, Y.-W.; Huang, M.-T.; Ho, C.-T.; Huang, Q. Enhancing anti-inflammation activity of curcumin through O/W nanoemulsions. *Food Chem.* **2008**, *108*, 419−424.

(22) Stepanek, P. Data analysis in dynamic light scattering. In *Dynamic Light Scattering*; Brown, W., Ed.; Oxford University Press: Oxford, U.K., 1993; pp 177−241.

(23) Lin, C.-C.; Lin, H.-Y.; Chen, H.-C.; Yu, M.-W.; Lee, M.-H. Stability and characterisation of phospholipid-based curcumin-encapsulated microemulsions. *Food Chem.* **2009**, *116*, 923−928.

(24) Pouton, C. W.; Porter, C. J. H. Formulation of lipid-based delivery systems for oral administration: Materials, methods and strategies. *Adv. Drug Delivery Rev.* **2008**, *60*, 625−637.

(25) Li, Y.; Zheng, J.; Xiao, H.; McClements, D. J. Nanoemulsion-based delivery systems for poorly water-soluble bioactive compounds: Influence of formulation parameters on polymethoxyflavone crystallization. *Food Hydrocolloids* **2012**, *27*, 517−528.

(26) Kaufman, V. R.; Garti, N. Effect of cloudy agents on the stability and opacity of cloudy emulsions for soft drinks. *J. Food Technol.* **1984**, *19*, 255−261.

(27) Kourniatis, L. R.; Spinelli, L. S.; Piombini, C. R.; Mansur, C. R. E. Formation of orange oil-in-water nanoemullsions using nonionic surfactant mixtures by high pressure homogenizer. *Colloid J.* **2010**, *72*, 396−402.

(28) Jafari, S.; He, Y.; Bhandari, B. Optimization of nano-emulsions production by microfluidization. *Eur. Food Res. Technol.* **2007**, *225*, 733−741.

(29) Yuan, Y.; Gao, Y.; Zhao, J.; Mao, L. Characterization and stability evaluation of β-carotene nanoemulsions prepared by high pressure homogenization under various emulsifying conditions. *Food Res. Int.* **2008**, *41*, 61−68.

(30) Qian, C.; McClements, D. J. Formation of nanoemulsions stabilized by model food-grade emulsifiers using high-pressure homogenization: Factors affecting particle size. *Food Hydrocolloids* **2011**, *25*, 1000−1008.
(31) Yuan, Y.; Gao, Y.; Mao, L.; Zhao, J. Optimisation of conditions for the preparation of β-carotene nanoemulsions using response surface methodology. *Food Chem.* **2008**, *107*, 1300−1306.
(32) Floury, J.; Desrumaux, A.; Legrand, J. Effect of ultra-high-pressure homogenization on structure and on rheological properties of soy protein-stabilized emulsions. *J. Food Sci.* **2002**, *67*, 3388−3395.
(33) Laguerre, M.; Lpez Giraldo, L. J.; Lecomte, J.; Figueroa-Espinoza, M.-C.; Bara, B.; Weiss, J.; Decker, E. A.; Villeneuv, P. Relationship between hydrophobicity and antioxidant ability of "phenolipids" in emulsion: A parabolic effect of the chain length of rosmarinate esters. *J. Agric. Food Chem.* **2010**, *58*, 2869−2876.
(34) Liu, W.; Guo, R. Interaction between flavonoid, quercetin and surfactant aggregates with different charges. *J. Colloid Interface Sci.* **2006**, *302*, 625−32.
(35) Di Mattia, C. D.; Sacchettia, G.; Mastrocolaa, D.; Pittia, P. Effect of phenolic antioxidants on the dispersion state and chemical stability of olive oil O/W emulsions. *Food Res. Int.* **2009**, *42*, 1163−1170.
(36) McClements, D. J. Crystals and crystallization in oil-in-water emulsions: Implications for emulsion-based delivery systems. *Adv. Colloid Interface Sci.* **2012**, *174*, 1−30.
(37) Wu, T.-H.; Yen, F.-L.; Lin, L.-T.; Tsai, T.-R.; Lin, C.-C.; Cham, T.-M. Preparation, physicochemical characterization, and antioxidant effects of quercetin nanoparticles. *Int. J. Pharm.* **2008**, *346*, 160−168.
(38) Garti, N.; Zakharia, I.; Spernath, A.; Yaghmur, A.; Aserin, A.; Hoffman, R.; Jacobs, L. Solubilization of water-insoluble nutraceuticals in nonionic microemulsions for water-based use. In *Trends in Colloid and Interface Science XVII*; Cabuil, V., Levitz, P., Treiner, C., Eds.; Progress in Colloid and Polymer Science, Vol. *126*; Springer: Berlin, 2004; pp 184−189.